Inorganic Chemistry

Communication

pubs.acs.org/IC

Going beyond Red with a Tri- and Tetracoordinate Boron Conjugate: Intriguing Near-IR Optical Properties and Applications in Anion Sensing

Samir Kumar Sarkar, Sanjoy Mukherjee, and Pakkirisamy Thilagar*

Department of Inorganic and Physical Chemistry, Indian Institute of Science, Bangalore 560012, India

Supporting Information

ABSTRACT: The design and synthesis of a new tri- and tetracoordinate boron conjugate is reported. The conjugate shows broad near-IR emission (~625−850 nm) and is found to be a selective colorimetric and ratiometric sensor for fluoride ions.

In recent years, luminescent organic dyes have emerged as indispensable components of modern materials chemistry.[1] In particular, near-infrared (NIR) luminescent dyes have attracted a lot of attention compared to other classes of luminogens (e.g., blue/green emissive dyes) in view of their biological, photovoltaic, and optoelectronic applications.[2] NIR monitoring of any target analyte is a challenging task. In the past decade, tetracoordinate boron-containing styryl−BODIPY dyes, primarily developed by Daub et al.[3a] and Akkaya et al.,[3b,c] have emerged as a versatile class of NIR luminogens, which find applications in bioimaging, photodynamic therapy, molecular recognition, artificial light-harvesting systems, and organic optoelectronic devices.[3,4] BODIPYs have been the subject of extensive studies in the past few years owing to their inherent sharp absorption and emission bands, high quantum yields, high photostability, and ease of functionalization.[4,5]

Tricoordinate boron-containing triarylboranes (TABs) have also attracted significant attention in past few years mainly due to their potential applications in organic light-emitting diodes,[6,7a,b] anion sensing,[7c−f] and organic thin-film transistors,[7g] etc. In the absence of suitable donor units, TABs commonly show photoluminescence at the blue end of the visible spectrum.[6,7] However, the incorporation of TAB units in rationally designed molecular architectures can be employed to achieve functional luminescent materials with longer-wavelength emissions. In this regard, TAB-based donor−acceptors dyad/triads and polymeric systems have been studied.[6−8] In the present decade, the combination of tri- and tetracoordinate boron conjugates (TAB−BODIPY dyad/triad) has received considerable attention.[9] In 2008, Lee et al. reported the first borane−BODIPY conjugate, which shows borane-to-BODIPY energy transfer (ET), resulting in single-channel emission from the BODIPY moiety, and the ET process was also utilized for selective recognition of cyanide ions.[9a] Very recently in 2013, we demonstrated unique di- and tricolor emissive properties of borane−BODIPY conjugates and their applications as fluoride-selective fluorescent sensors.[9f,g] In spite of these efforts, TAB-based NIR luminogens are not well documented in the literature. An important objective of this project is to develop TAB-based NIR materials and utilization of their properties for potential applications.

In the present study, we considered decoration of a styryl−BODIPY moiety with TAB units to be a rational approach for achieving NIR-emissive TABs. Also, we reasoned that the incorporation of an iodothiophene moiety at the meso position of the BODIPY unit may lengthen effective conjugation and provide sites for further functionalization. Accordingly, we designed and synthesized a $(TAB)_2$−styryl−BODIPY conjugate (**1**) (Scheme 1; see the Supporting Information, SI). To understand the effects of TAB entities on the optical properties of **1**, model system **2** (Scheme 1) was also synthesized and studied (see the SI). Compounds **1** and **2** were synthesized using the procedure shown in Scheme 1. Condensation of 5-iodothiophene-2-carbaldehyde (**1a**) with 2-methylpyrrole, followed by oxidation with 2,3-dichloro-5,6-dicyano-1,4-benzoquinone (DDQ) and the subsequent addition of Et_3N and $BF_3{\cdot}Et_2O$ in CH_2Cl_2, gave **1b**. Further, condensation of **1b** with 4-(dimesitylboryl)benzaldehyde (or benzaldehyde for **2**) in the presence of *p*-toluenesulfonamide (PTSA) and piperidine resulted in compound **1**. Compound **1** was characterized by NMR (^1H, ^{13}C, and ^{19}F) and MALDI-TOF techniques (see the SI). The molecular structure of **1** was confirmed by single-crystal X-ray diffraction (Figure 1) studies.

Scheme 1. Synthesis of 1[a]

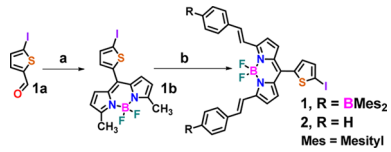

[a](a) 2-Methylpyrrole/DCM, DDQ, Et_3N, and $BF_3{\cdot}Et_2O$. (b) 4-(Dimesitylboryl)benzaldehyde (**1**) or benzaldehyde (**2**), piperidine, and PTSA/toluene.

The molecular structure of **1** is shown in Figure 1. The molecule adopts a "Y" shape with spatially separated TAB units [the $B_2(TAB)$−$B_3(TAB)$ distance is 12.69 Å]. The boradiazaindacene unit forms a near-planar arrangement with the two Ar_3B planes (dihedral angles of 13.0 and 20.2°). Density functional theory (DFT; B3LYP)[10] calculations almost reproduce the structure determined experimentally (see the SI).

Received: September 26, 2013
Published: February 13, 2014

dx.doi.org/10.1021/ic402441w | *Inorg. Chem.* 2014, 53, 2343−2345

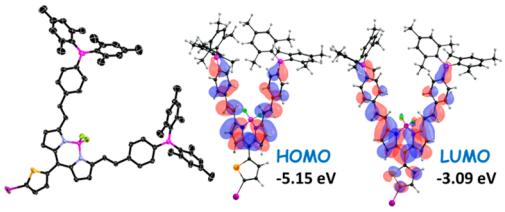

Figure 1. Thermal ellipsoid probability plot of **1** (left, thermal ellipsoids are at a 30% probability level) and FMOs of **1** (isovalue = 0.02). Color code: C, black; B, magenta; N, blue; F, green; S, yellow; I, purple.

The absorption spectrum of **1** (SI, Figure S24) shows bands at ~400 ($\varepsilon = 5.15 \times 10^4$), ~480 ($\varepsilon = 1.56 \times 10^4$), ~615 ($\varepsilon = 4.5 \times 10^4$), and ~675 nm ($\varepsilon = 1.06 \times 10^5$). TAB units in conjugate **1** cause a red shift of ~15−25 nm with respect to **2**. This red shift possibly results from the lower HOMO−LUMO gap induced by the TAB (2.06 eV) in **1** compared to that in **2** (2.12 eV), as shown by DFT calculations (Figure 1 and the SI). The nonlocalized distribution of the frontier molecular orbitals (FMOs; Figure 1 and the SI) over the molecular framework is indicative of effective conjugation in **1**. Compound **1** shows stronger absorption characteristics in the region ~350−450 nm ($\varepsilon = 5.15 \times 10^4$ at λ_{abs} = 400 nm) compared to **2** ($\varepsilon = 2.75 \times 10^4$ at λ_{abs} = 400 nm). The difference in the absorption characteristics can be attributed to the presence of a TAB unit in **1**. Time-dependent DFT (TD-DFT) calculations suggest that the ~400 nm band in **1** is dominated by the transition from the styryl−BODIPY-centered HOMO to the boryl-centered LUMO+1 (f = 1.1010) level (see the SI).

When conjugate **2** is excited at 400 nm, the emission spectrum shows a sharp band at ~675 nm with a shoulder at ~720 nm (Figure S24). Upon excitation at 400 nm, **1** shows a sharp emission peak at ~700 nm with two shoulders at ~625 and ~755 nm. The emission bands of **1** are ~25 nm red-shifted compared to **2** (λ_{em} = 675 nm). The bathochromic shift is due to the involvement of low-energy FMOs in **1** compared to **2**. This inference is supported by computational studies. Time-resolved emission decay profiles (λ_{em} = 700 nm) show that **1** has an excited-state fluorescence lifetime of 3.2 ns, evidently suggesting the nature of this luminescence as fluorescence (see the SI). The emission wavelengths (λ_{em}) for compounds **1** and **2** are unaffected in a wide range of concentrations, signifying the absence of any intermolecular interactions (see the SI). The absorption and emission features of **1** (and **2**) are also insensitive to the solvent polarity (see the SI), indicating the absence of any intramolecular charge-transfer (ICT) processes. Although excitations at different spectral regions (λ_{ex}) alter the emission intensities of **1**, they do not affect λ_{em} (see the SI). Interestingly, upon excitation (λ_{ex}) at 375−400 nm, compound **1** shows the highest intense emission bands (see the SI). As stated vide supra, TD-DFT studies and a comparison with **2** indicate that the ~375−400 nm absorption bands in **1** are dominated by the Ar_3B-centered transitions (Figure S24 and the SI). The results show that a highly efficient electronic energy-transfer (EET) process (from TAB to BODIPY) is present in **1**, which may be facilitated by the near-coplanar orientations of the styryl−BODIPY core and pendant Ar_3B units. This borane-to-BODIPY ET, which can be considered to involve a Foster resonance energy-transfer (FRET) process, is probably responsible for the absence of any higher-energy Ar_3B-centered emission, which is in contrast to the previously reported meso-substituted dual-emissive borane−BODIPY conjugates.[9f] The excitation spectrum of **1** (λ_{em} = 700 nm) duplicates its absorption spectrum, which strongly supports our previous argument.

Consecutively, we became interested in exploring its potential as an anion sensor. Compound **1** was found to be selectively responsive toward fluoride ions. Fluoride plays both an advantageous (e.g., dental care, anesthetics, osteoporosis, and psychiatric drugs) and injurious (e.g., water contamination, etc.) role in health care and environment.[11a] In this context, colorimetric and NIR recognition of fluoride has become an important issue to address.[11] To evaluate the fluoride binding ability of **1**, it was titrated against tetra-*n*-butylammonium fluoride [TBAF; in a 10 μM dichloromethane (DCM) solution]. Conjugate **1** shows colorimetric as well as ratiometric fluorescent response in the presence of fluoride (Figure 2).

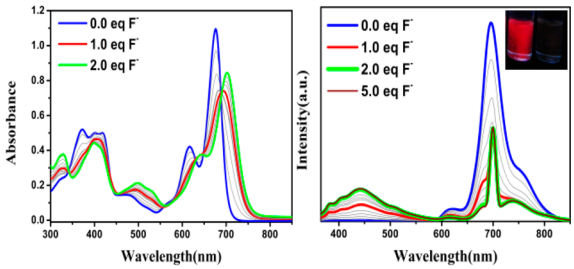

Figure 2. Absorption and emission (10 μM DCM solution, λ_{ex} = 350 nm) spectral changes of **1** upon addition of TBAF. The residual signal 700 nm is the overtone of excitation (350 nm).

The addition of fluoride to compound **1** causes a considerable red shift in its absorption spectrum. The characteristic styryl−BODIPY band is shifted from ~675 to ~700 nm. The absorption bands at ~325 and ~500 nm gradually gain in intensity. Further, the characteristic boryl absorption band at ~400 nm shows partial quenching. Saturation of these optical responses occurs after the addition of ~2.0 equiv of fluoride, indicating the formation of a 1:2 complex. The overall fluoride association constant (K_2) for compound **1** was found to be 8.87×10^9. The changes in the absorption spectrum result in a visually observable color change from dark green to light greenish-yellow in the solution state. However, the appearance of any characteristic ICT band was not observed. TD-DFT studies (see the SI) show that the ~500 nm band arises from the fluoride-bound borane-centered HOMO−5 to styryl-centered LUMO (568.32 nm; f = 0.3689). DFT studies (see the SI) also suggest that the addition of fluoride to the TAB entity (forming **1**·2F⁻) results in a significant lowering of the HOMO−LUMO gap, although the FMOs are delocalized over the entire molecular backbone, indicating the absence of any possible ICT processes in **1**·2F⁻.

Conjugate **1** (in a 10 μM DCM solution) shows a ratiometric fluorescent response upon the addition of fluoride (Figure 3).

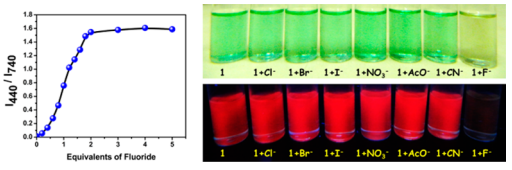

Figure 3. Ratiometric fluorescence response (I_{440}/I_{740} in a 10 μM DCM solution; λ_{ex} = 350 nm) of **1** upon the addition of TBAF in a 10 μM DCM solution (left). Photographs of **1** under ambient light (right top) and UV light (right bottom) in the presence of different species.

dx.doi.org/10.1021/ic402441w | Inorg. Chem. 2014, 53, 2343−2345

With the gradual addition of TBAF, the broad emission bands at ~625−800 nm display significant quenching (Stern−Volmer quenching constant K_{sv} = 3.7 × 10^7). The quenching of this emission band may possibly occur from the stopping of the EET process from the TAB moiety to BODIPY fluorophore. Interestingly, a distinctly new broad emission band appears at ~400 nm and gradually increases upon the addition of fluoride. Dual-emissive behavior is prominent in the fluoride-bound form **1**·2F$^-$ rather than in the free form (**1**). This dual emission possibly results from the diminished EET processes (from the fluoride-bound TAB units to the BODIPY core) in **1**·2F$^-$, allowing emission from higher-energy states. The saturation of emission occurs upon the addition of 2.0 equiv of fluoride. Such a high sensitivity is uncommon in other TAB-based fluoride receptors. During fluoride addition, monitoring the I_{440}/I_{740} ratio (Figure 3) clearly demonstrates the ratiometric-response behavior of **1**. The I_{440}/I_{740} intensity ratio is initially 0.0, which gradually increase to ~1.5 and reaches saturation after the addition of only 2.0 equiv of fluoride. This type of ratiometric response provides the opportunity in molecular sensors to intrinsically rectify measurement errors. The plot also suggests the absence of any significant negative cooperative bonding effect after the addition of 1.0 equiv of fluoride. Such behavior may be rationalized considering the spatial separation of the two TAB units and the absence of any strong donor−acceptor ICT process, which affect the binding of the second fluoride anion. Competitive binding studies (Figure 3 and the SI) demonstrate that the photophysical response of conjugate **1** is highly selective toward fluoride. Interestingly, **1** is insensitive even toward the presence of large quantities of CN$^-$ (>10.0 equiv), which is a general interfering species in TAB-based anion receptors. The ^{1}H NMR titrations reveal that while compound **1** binds with fluoride anions, it remains practically inert toward the presence of even large amounts of cyanide anions (see the SI).

In conclusion, we have developed a NIR-emitting TAB-decorated styryl−BODIPY (**1**) via a facile synthetic route. The incorporation of TAB entities results in a significantly red-shifted broad emission in **1** (compared to **2**). The near-coplanar orientation of Ar_3B planes the BODIPY core results in a highly efficient (TAB-to-BODIPY) EET process in **1**. Conjugate **1** acts as a highly selective and sensitive fluoride sensor with a naked eye visual response as well as ratiometric fluorescent response. The dual emission in fluoride-bound **1** possibly results from the restricted partial TAB-to-BODIPY ET. Further investigations are underway.

■ ASSOCIATED CONTENT

Supporting Information

Synthesis, characterizations, and computational data. This material is available free of charge via the Internet at http://pubs.acs.org.

■ AUTHOR INFORMATION

Corresponding Author

*E-mail: thilagar@ipc.iisc.ernet.in. Tel: 0091-80-22933353. Fax: 0091-80-23601552.

Notes

The authors declare no competing financial interest.

■ ACKNOWLEDGMENTS

P.T. thanks the DST and CSIR, New Delhi, for financial support. S.K.S. thanks IISc, and S.M. thanks the CSIR for SPMF.

■ REFERENCES

(1) (a) Binnemans, K. *Chem. Rev.* **2009**, *109*, 4283. (b) Freeman, R.; Willner, B.; Willner, I. *J. Phys. Chem. Lett.* **2011**, *2*, 2667. (c) Sasabe, H.; Kido, J. *Chem. Mater.* **2011**, *23*, 621. (d) Li, D.; Zhang, H.; Wang, Y. *Chem. Soc. Rev.* **2013**, *42*, 8416. (e) Wang, X.; Wolfbeis, O. S.; Meier, R. J. *Chem. Soc. Rev.* **2013**, *42*, 7834. (f) Wu, P.; Yan, X.-P. *Chem. Soc. Rev.* **2013**, *42*, 5489. (g) Bruel, A. M.; Hager, M. D.; Schubert, U. S. *Chem. Soc. Rev.* **2013**, *42*, 5366. (h) Ciardelli, F.; Ruggeri, G.; Pucci, A. *Chem. Soc. Rev.* **2013**, *42*, 857. (i) Huang, X.; Han, S.; Huang, W.; Li, X. *Chem. Soc. Rev.* **2013**, *42*, 173.

(2) (a) Luo, S.; Zhang, E.; Su, Y.; Cheng, T.; Shi, C. *Biomaterials* **2011**, *32*, 7127. (b) Pansare, V. J.; Hejazi, S.; Faenza, W. J.; Prud'homme, R. K. *Chem. Mater.* **2012**, *24*, 812. (c) Xiang, H.; Cheng, J.; Ma, X.; Zhou, X.; Chruma, J. J. *Chem. Soc. Rev.* **2013**, *42*, 6128.

(3) (a) Rurack, K.; Kollmannsberger, M.; Daub, J. *New J. Chem.* **2001**, *25*, 289. (b) Atilgan, S.; Ekmekci, Z.; Dogan, A. L.; Guc, D.; Akkaya, E. U. *Chem. Commun.* **2006**, 4398. (c) Buyukcakir, O.; Bozdemir, O. A.; Kolemen, S.; Erbas, S.; Akkaya, E. U. *Org. Lett.* **2009**, *11*, 4644.

(4) (a) Ozlem, S.; Akkaya, E. U. *J. Am. Chem. Soc.* **2009**, *131*, 48. (b) Atilgan, S.; Ozdemir, T.; Akkaya, E. U. *Org. Lett.* **2008**, *10*, 4065. (c) Ela, S. E.; Yilmaz, M. D.; Icli, B.; Dede, Y.; Icli, S.; Akkaya, E. U. *Org. Lett.* **2008**, *10*, 3299. (d) Bura, T.; Leclerc, N.; Fall, S.; Leveque, P.; Heiser, T.; Ziessel, R. *Org. Lett.* **2011**, *13*, 6030. (e) Bura, T.; Leclerc, N.; Fall, S.; Léveque, P.; Heiser, T.; Retailleau, P.; Rihn, S.; Mirloup, A.; Ziessel, R. *J. Am. Chem. Soc.* **2012**, *134*, 17404.

(5) (a) Loudet, A.; Burgess, K. *Chem. Rev.* **2007**, *107*, 4891. (b) Ulrich, G.; Harriman, A.; Ziessel, R. *Angew. Chem., Int. Ed.* **2008**, *47*, 1202.

(6) (a) Yamaguchi, S.; Akiyama, S.; Tamao, K. *J. Am. Chem. Soc.* **2001**, *123*, 11372. (b) Yamaguchi, S.; Shirasaka, T.; Akiyama, S.; Tamao, K. *J. Am. Chem. Soc.* **2002**, *124*, 8816. (c) Sundararaman, A.; Victor, M.; Varughese, R.; Jäkle, F. *J. Am. Chem. Soc.* **2005**, *127*, 13748. (d) Chiu, C.-W.; Gabbaï, F. P. *J. Am. Chem. Soc.* **2006**, *128*, 14248. (e) Liu, X.-Y.; Bai, D.-R.; Wang, S. *Angew. Chem., Int. Ed.* **2006**, *45*, 5475. (f) Parab, K.; Venkatasubbaiah, K.; Jäkle, F. *J. Am. Chem. Soc.* **2006**, *128*, 12879. (g) Sakuda, E.; Funahashi, A.; Kitamura, N. *Inorg. Chem.* **2006**, *45*, 10670. (h) Yuan, M.-S.; Liu, Z.-Q.; Fang, Q. *J. Org. Chem.* **2007**, *72*, 7915. (i) Bai, D.-R.; Liu, X.-Y.; Wang, S. *Chem.—Eur. J.* **2007**, *13*, 5713. (j) Zhao, S.-B.; McCormick, T.; Wang, S. *Inorg. Chem.* **2007**, *46*, 10965. (k) Kim, Y.; Gabbaï, F. P. *J. Am. Chem. Soc.* **2009**, *131*, 3363.

(7) (a) Entwistle, C. D.; Marder, T. B. *Chem. Mater.* **2004**, *16*, 4574. (b) Yamaguchi, S.; Wakamiya, A. *Pure Appl. Chem.* **2006**, *78*, 1413. (c) Wade, C. R.; Gabbai, F. P. *Dalton Trans.* **2009**, 9169. (d) Hudnall, T. W.; Chiu, C.-W.; Gabbai, F. P. *Acc. Chem. Res.* **2009**, *42*, 388. (e) Wade, C. R.; Broomsgrove, A. E. J.; Aldridge, S.; Gabbai, F. P. *Chem. Rev.* **2010**, *110*, 3958. (f) Kim, Y.; Huh, H.-S.; Lee, M. H.; Lenov, I. L.; Zhao, H.; Gabbai, F. P. *Chem.—Eur. J.* **2011**, *17*, 2057. (g) Huang, W.; Besar, K.; LeCover, R.; Rule, A. M.; Breysse, P. N.; Katz, H. E. *J. Am. Chem. Soc.* **2012**, *134*, 14650.

(8) (a) Hudson, Z. M.; Wang, S. *Acc. Chem. Res.* **2009**, *42*, 1584. (b) Jäkle, F. *Chem. Rev.* **2010**, *110*, 3985. (c) Tanaka, K.; Chujo, Y. *Macromol. Rapid Commun.* **2012**, *33*, 1235.

(9) (a) Huh, J. O.; Do, Y.; Lee, M. H. *Organometallics* **2008**, *27*, 1022. (b) Fu, G.-L.; Pan, H.; Zhao, Y.-H.; Zhao, C.-H. *Org. Biomol. Chem.* **2011**, *9*, 8141. (c) Sun, H.; Dong, X.; Liu, S.; Zhao, Q.; Mou, X.; Yang, H. Y.; Huang, W. *J. Phys. Chem. C* **2011**, *115*, 19947. (d) Yin, Z.; Tam, A. Y.-Y.; Wong, K. M.-C.; Tao, C.-H.; Li, B.; Poon, C.-T.; Wu, L.; Yam, V. W.-W. *Dalton Trans.* **2012**, *41*, 11340. (e) Lu, J.; Ko, S.-B.; Walters, N. R.; Wang, S. *Org. Lett.* **2012**, *14*, 5660. (f) Swamy, P. C. A.; Mukherjee, S.; Thilagar, P. *Chem. Commun.* **2013**, *49*, 993. (g) Sarkar, S. K.; Thilagar, P. *Chem. Commun.* **2013**, *49*, 8558.

(10) Frisch, M. J.; et al. *Gaussian 09*; Gaussian Inc.: Wallingford, CT, 2009 (see the SI for complete citation).

(11) (a) Jagtap, S.; Yenkie, M. K.; Labhsetwar, N.; Rayalu, S. *Chem. Rev.* **2012**, *112*, 2454. (b) Cametti, M.; Rissanen, K. *Chem. Soc. Rev.* **2013**, *42*, 2016.